DOI: 10.1002/ejic.200600865

The Electrochemical Behaviour of Organonickel Complexes: Mono-, Di- and Trivalent Nickel

Axel Klein,*[a] André Kaiser,[a] Biprajit Sarkar,[b] Matthias Wanner,[b] and Jan Fiedler[c]

Keywords: Electron transfer / Nickel / Electrochemistry / EPR spectroscopy / Spectroelectrochemistry

The redox properties of organometallic nickel complexes of the type [(α-diimine)Ni(Mes)Br], [(α-diimine)Ni(Mes)$_2$] and the complexes *trans*-[(PPh$_3$)$_2$Ni(Mes)Br] and *trans*-[(PPh$_3$)$_2$-Ni(Fmes)Br] [Mes = mesityl (2,4,6-trimethylphenyl); Fmes = tris(2,4,6-trifluoromethyl)phenyl] have been studied in detail by various electrochemical and spectroelectrochemical (UV/Vis/NIR and EPR) methods. Upon electrochemical reduction, the bromido mesityl derivatives undergo cleavage of the bromide ligand. The resulting reactive species and their products from follow-up reactions are investigated. Electrochemical oxidation leads to formally trivalent nickel species. The metal contribution to the unpaired electron for the formally monovalent and trivalent nickel species can be estimated from EPR spectroscopy.

Introduction

Organonickel(II) complexes are widely used in organometallic catalysis. One of the first benchmarks in that field were the nickel phosphane complexes used in the Shell higher olefin process (SHOP).[1] In the last decade the interest in organonickel catalysts has mainly focused on nickel diimine complexes. Highly reactive catalysts for olefin polymerisation have been developed on the basis of methylnickel complexes of various diimine ligands, mainly by Brookhart.[2] The active catalyst species were found to be mainly cationic complexes of the type [(N^N)Ni(R)L]$^+$ (N^N = α-diimine; L = easily replaceable ligand). Furthermore, nickel diimine complexes have gained an enormous interest in electrocatalytic applications[3] such as electrocatalytic C–C or C–P coupling reactions with various aryl, vinyl or alkyl halides R–X (see Scheme 1),[4–7] homogeneous electromediated reduction (HEMR) of olefins, ketones or alkyl halides,[8–10] electrochemical carboxylation of bromostyrenes[11] or aziridines,[12] electroreductive carbonylation of organic halides[13] and electroreductive coupling of olefins and polyhalo compounds.[14]

A mechanism for the C–C coupling reactions was initially proposed by Amatore and Jutand[15] for the corresponding diphosphane (dppe) complexes and was subsequently established for 2,2′-bipyridine-containing systems

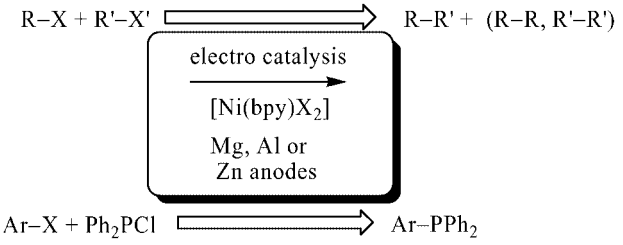

Scheme 1. Electrocatalytic C–C or C–P coupling reactions of aryl, vinyl or alkyl halides.

mainly based on kinetic investigations.[6,16,17] For a system starting from [(bpy)NiX$_2$] (X = halide) pre-catalysts it can be depicted as in Scheme 2.

In addition to these kinetic investigations, the oxidative addition reaction of ArBr to zero-valent nickel species formed in situ as the first part of the catalytic cycle has been proved by preparative electrochemistry. Thus, the oxidative addition of aryl halides to species formed upon electrochemical reduction of [(bpy)$_n$NiX$_2$] (n = 1–3; X = Br, BF$_4$) leads to the nickel(II) complexes [(bpy)Ni^{II}(Ar)Br] in reasonably high yields.[18,19] The complex [(bpy)Ni(Mes)Br], which is an excellent catalyst precursor for the oligomerisation of ethylene, is obtained from [(bpy)NiBr$_2$] and MesBr in 87% yield.[18]

The subsequent steps of the proposed catalytic cycle comprise a single electron transfer and subsequent scission of the bromide ligand to give the monovalent species [(bpy)-Ni^{I}(Ar)]. Oxidative addition of RX then leads to trivalent pentacoordinate [(bpy)Ni^{III}(Ar)(R)X], which finally eliminates the coupling product ArR. The resulting nickel(I) species is then reduced to the aforementioned nickel(0) catalyst [(bpy)Ni^0]. So far very little preparative or spectroscopic

[a] Universität zu Köln, Institut für Anorganische Chemie, Greinstraße 6, 50969 Köln, Germany
E-mail: axel.klein@uni-koeln.de
[b] Universität Stuttgart, Institut für Anorganische Chemie, Pfaffenwaldring 55, 70569 Stuttgart, Germany
[c] J. Heyrovský Institute of Physical Chemistry, Academy of Sciences of the Czech Republic, Dolejškova 3, 18 000 Prague 8, Czech Republic

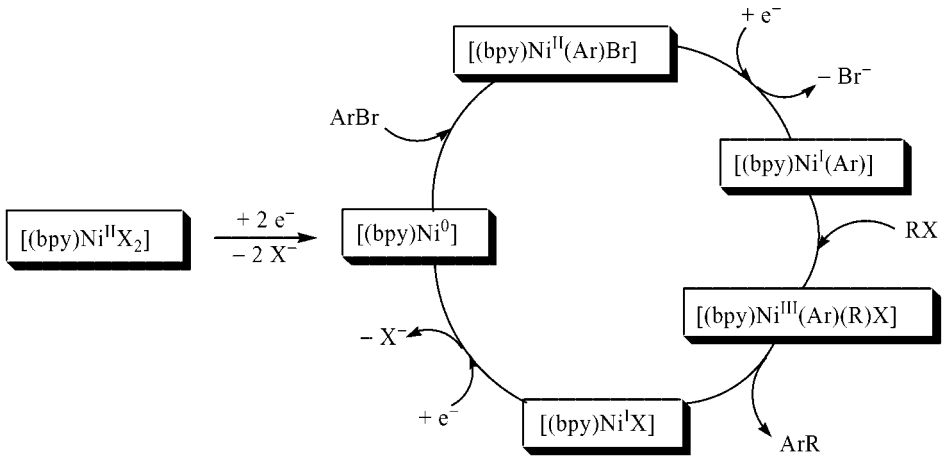

Scheme 2. Proposed mechanism for the C–C coupling reactions.

evidence has been published for this part. The NMR spectroscopic data of the proposed nickel(III) species [(bpy)-Ni(Mes)$_2$Br] have been reported,[19] but these data do not show any sign of paramagnetic shifts, and the characterisation of these species by EPR spectroscopy was not performed. No spectroscopic evidence has been found so far for the nickel(I) species in the next catalytic step.

To explore the mechanism of this interesting electrocatalytic reaction in further details we have started an investigation on the electrochemistry of a number of mesitylnickel complexes of various α-diimine ligands [(N^N)Ni(Mes)Br], thus starting at the point of the proposed cycle which has remained largely unclear so far. We have used spectroelectrochemical methods (UV/Vis/NIR and EPR) to characterise the resulting species as these techniques allow the in situ generation and spectroscopic characterisation of labile or even transient species.[20]

The complexes [(N^N)Ni(Mes)Br] used in this investigation, with the α-diimine ligands depicted in Scheme 3, have been described in preliminary detailed studies using optical spectroscopy, XRD and EXAFS spectroscopy in combination with quantum chemical calculations.[21–23] It was shown that the LUMOs were mainly localised in the diimine π* levels, which means that the diimine ligands should be largely involved in electrochemical reduction of these complexes. Since the splitting of the bromide ligand is presumed from the reduced states of these complexes, the related dimesityl complexes [(N^N)Ni(Mes)$_2$], which have been described recently,[21,23] were also included in this study. For further comparison we also incorporated the complex *trans*-[(PPh$_3$)$_2$Ni(Mes)Br], which usually serves as a precursor to the title complexes,[22,23] and the perfluorinated derivatives *trans*-[(PPh$_3$)$_2$Ni(Fmes)Br] and [(bpy)-Ni(Fmes)Br] [Fmes = nonafluoromesityl = 2,4,6-tris(trifluoromethyl)phenyl], the preparation and analytical data of which are given in the Experimental Section.

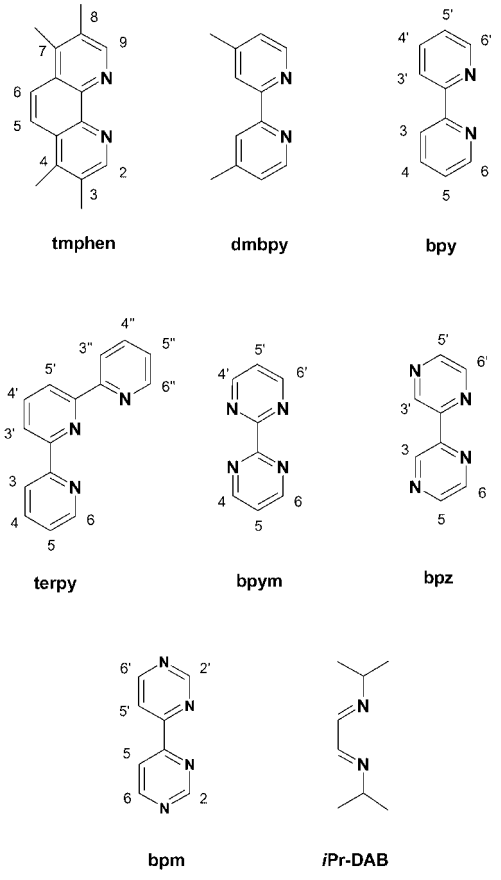

Scheme 3. Diimine ligands (N^N). tmphen = 3,4,7,8-tetramethyl-1,10-phenanthroline, dmbpy = 4,4′-dimethyl-2,2′-bipyridine, bpy = 2,2′-bipyridine, terpy = 2,2′,6′′-terpyridine, bpym = 2,2′-bipyrimidine, bpz = 2,2′-bipyrazine, bpm = 4,4′-bipyrimidine, *i*Pr-DAB = *N*,*N*′-diisopropyl-1,2-ethanediimine (*N*,*N*′-diisopropyl-1,4-diazabutadiene).

Results and Discussion

Electrochemistry

Reduction Reactions

The bromido mesityl complexes [(N^N)Ni(Mes)Br] exhibit rather complex electrochemical behaviour at 298 K, as shown in Figure 1 (data summarised in Table 1).

After a first irreversible reduction wave (E_{R1}) we observe a reversible wave E_2 (E_{R2}/E_{O2}) for the more basic ligands tmphen, dmbpy and bpy. The cathodic peak potentials E_{R1} and E_{R2} increase (shift positively) along the series tmphen > dmbpy > bpy > bpym > bpz > *i*Pr-DAB > bpm. Since the values for E_{R2} increase more rapidly, E_{R1} and E_{R2} overlap partially at the lower end of the series, starting from bpym. Here, square-wave voltammetry helped to determine the individual values. This series represents the decreasing basicity or increasing π-accepting ability (in accordance with the low-lying π* LUMOs) of the diimine ligand. On the reverse scan a re-oxidation wave ($E_{O1'}$) is observed at around –1 V. The two reduction waves are followed by further waves that are partly reversible (E_{R3}) for the less basic ligands. An exception for this complex behaviour can be observed for the terpy complex $[(terpy)Ni(Mes)]^+$, for which two reversible reduction waves are found. The corresponding dimesityl complexes $[(N^N)Ni(Mes)_2]$ also exhibit full reversibility of the first two reduction processes (Figure 2, Table 2). Since no bromide co-ligand is present in these systems a first strong evidence emerges that the splitting of the bromide from the complexes [(N^N)Ni(Mes)Br] after the first reduction reaction is the reason for their complicated behaviour. This splitting reaction has been proposed before by others,[16,18,19] but no convincing proof was provided.

At low temperature (213 K) the situation is altered. For the dmbpy complex a re-oxidation E_{O1} to the first electrochemical process (E) is observed. At normal scan rates the ratio I_{pa}/I_{pc} is less than 1, although it reaches unity when scanned at rates above 500 mV s^{-1}. For the complexes with bpy (Figure 3), bpym, *i*Pr-DAB and bpm the process E_1 (E_{R1}/E_{O1}) is fully reversible even at normal scan rates. Com-

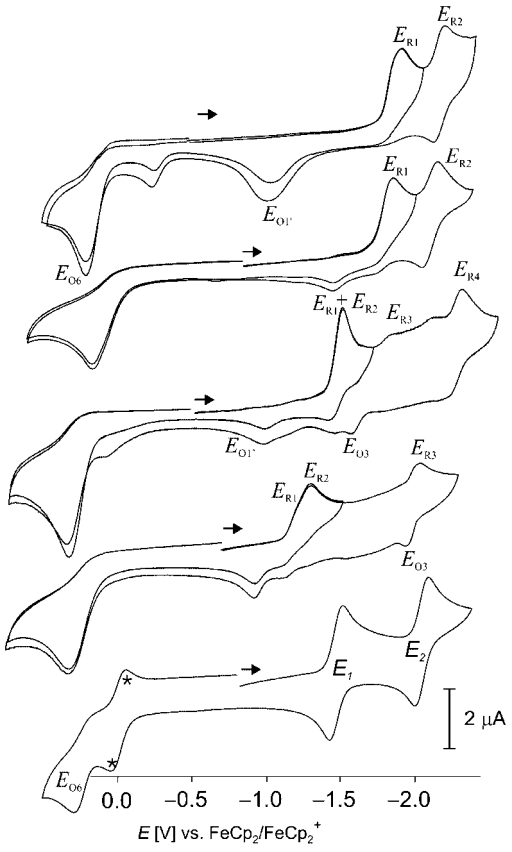

Figure 1. Cyclic voltammograms of [(tmphen)Ni(Mes)Br], [(dmbpy)Ni(Mes)Br], [(bpym)Ni(Mes)Br] (in thf), [(bpz)Ni(Mes)-Br] and $[(terpy)Ni(Mes)]^+$ (from top to bottom), in dmf/Bu_4NPF_6 solution at 298 K; * marks the redox waves of the ferrocene/ferrocenium standard.

Table 1. Electrochemical data of the bromido(mesityl)nickel complexes [(N^N)Ni(Mes)Br].[a]

(N^N)	E_{O6}	$E_{O1'}$	$E_{R1\ (irr.)}$ or E_1 (ΔE_{pp})	$E_{R2\ (irr.)}$ or E_2 (ΔE_{pp})	$E_{R2'\ (irr.)}$ or E_3 (ΔE_{pp})	$E_{R3\ (irr.)}$ or E_3 (ΔE_{pp})	$E_{R1} - E_{R1(L)}$	T [K]
tmphen	0.16	–1.51	–1.94 irr.	–2.18 (78)	–	–2.84 irr.	0.72	298
tmphen	0.27	–1.27	–2.00 irr	–2.16 (64)	–	–2.90 irr.	0.54	213
dmbpy	0.18	–1.47	–1.86 irr.	–2.08 (76)	–	–2.85 irr.	0.80	298
dmbpy	0.42	–	–1.87 (76)	–2.10 irr.	–2.58 irr.	–2.85 (91)	0.79	213
bpy	0.25	–1.45	–1.85 irr.	–2.00 (71)	–	–2.61 irr.	0.74	298
bpy	0.45	–	–1.79 (73)	–1.94 irr.	–2.65 (91)	–2.83 irr.	0.80	213
bpym	0.31	–1.04	–1.49 irr.	–1.58 irr.	–	–2.42 (96)	0.77	298
bpym	0.52	–	–1.47 (60)	–1.53 (81)	–2.22 (83)	–2.46 irr.	0.79	213
*i*Pr-DAB	0.30	–0.93	–1.34 irr.	–1.46 irr.	–	–2.10 irr.	1.30	298
*i*Pr-DAB	0.43	–	–1.37 (74)	–1.56 irr.	–	–2.45 irr.	1.27	213
bpz	0.29	–0.87	–1.31 irr.	–1.36 irr.	–	–2.02 irr.	0.77	298
bpz	0.37	–	–1.34 (75)	–	–1.88 (86)	–2.11 irr.	0.74	213
bpm	0.30	–0.67	–1.25 irr.	–	–	–1.91 (88)	0.61	298
bpm	0.29	–	–1.20 (66)	–	–1.82 (92)	–1.92 (92)	0.66	213
terpy	0.28	–	–1.45 (78)	–2.03 (81)	–	–2.79 (99)	1.04	298

[a] From cyclic voltammetry or square-wave voltammetry in 0.1 M dmf/Bu_4NPF_6 solutions. Scan rate: 100 mV s^{-1}. Potentials (E) in V vs. ferrocene/ferrocenium. Reduction potentials E_{R1}, E_{R2} and E_{R3} are cathodic peak potentials for irreversible waves. E_1 and E_2 are half-wave potentials for reversible waves, with the peak-to-peak separation ΔE_{pp} in mV given in parentheses. Oxidation potentials are given as anodic peak potentials.

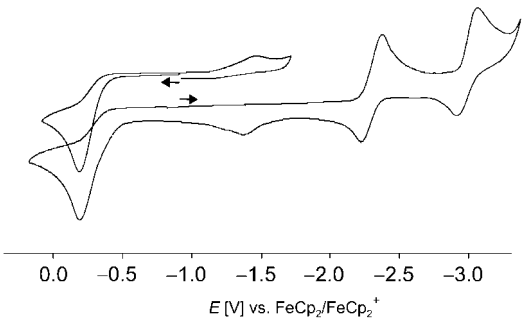

Figure 2. Cyclic voltammograms of [(bpy)Ni(Mes)$_2$] in thf/Bu_4NPF_6; scan rate: 100 mV s^{-1} at 298 K.

pared to measurements at 298 K, the peaks E_{R2} and E_{R3} are much smaller and further small reduction waves, for example $E_{R2'}$, are observed. We can therefore conclude that E_2 and E_3 are processes that are due to products emerging from the first electrochemical reduction (E) followed by a chemical reaction (C; EC mechanism). Evidence that the C process is the cleavage of Br^- thus comes from the reversible behaviour of the terpy complex, the dimesityl complexes (Figure 2, Table 2) and, as tested subsequently, from the increasing reversibility of the E_1 process upon addition of an excess of Bu_4NBr. Such an EC mechanism has been established for a number of diimine complexes of other transition metals such as Ru, Os, Rh, Ir or Re with halide coligands,[20b,24–26] and also for related phosphane complexes of Pd and Ni.[27]

If we examine the details further we find that in comparison to the dimesityl complexes the first reduction potentials of the bromido mesityl complexes are shifted to less negative values and that within the series of complexes the potentials depend strongly on the nature of the diimine ligand. Quantitative measurements using the Baranski method[28] revealed two successive one-electron reductions for the dimesityl complexes. Polarographic measurements on the bromido mesityl complexes also confirmed the uptake of one electron for the E_{R1} process. Other studies have shown that in the presence of additional MesBr the first reduction wave of [(bpy)Ni(Mes)Br] comprises two electrons and the complex [(bpy)Ni(Mes)$_2$] is formed under these conditions.[16,18,19] Corresponding experiments by us confirm these results. However, without additional MesBr only small amounts of the dimesityl complexes are formed during the reduction, therefore these species cannot account for the reversible waves E_2.

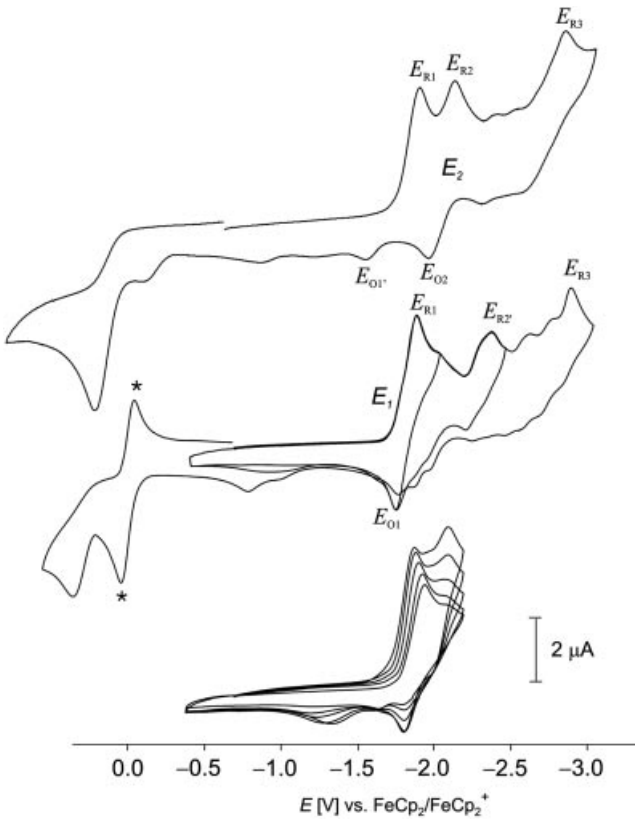

Figure 3. Cyclic voltammograms of [(bpy)Ni(Mes)Br] in thf/Bu_4NPF_6 solution at 298 K (top), in dmf/Bu_4NPF_6 solution at 238 K (middle), and dmf/Bu_4NPF_6 solution at temperatures varying between 238 and 278 K (bottom); * marks the redox waves of the ferrocene/ferrocenium standard.

The reductive electrochemistry of the perfluorinated derivative [(bpy)Ni(Fmes)Br] occurs at much less negative potential, as expected due to the presence of the electron-withdrawing F substituents (Table 3). Under normal experimental conditions (scan rate: 100 mV s^{-1} at 298 K) the first wave appears almost reversible (ΔE_{pp} = 66 mV; peak-current ratio = 0.91). This is interesting, since the use of very poor bases like *i*Pr-DAB or bpz also increases the reduction potential but does not lead to reversible behaviour to the same extent. Obviously, the rate of bromide splitting depends on the net electron density on the nickel atom, which is not

Table 2. Electrochemical data of dimesitylnickel complexes [(N^N)Ni(Mes)$_2$].[a]

(N^N)	E_{O1}	E_1 (ΔE_{pp})	E_2 (ΔE_{pp})	E_{R3}	$\Delta E_1 - E_2$	$\Delta E_1 - E_1(L)$	Solvent
tmphen	–0.23	–2.42 (75)	–3.11 (105)	–3.40	0.69	0.26	thf
tmphen	–0.25	–2.22 (73)	–2.97 irr.	–3.33	0.75	0.46	dmf
bpy	–0.14	–2.19 (87)	–2.97 (99)	–	0.78	0.58	thf
bpy	–0.19	–2.02 (71)	–2.89 (89)	–3.08	0.87	0.55	dmf
bpz	0.09	–1.61 (72)	–2.53 (92)	–3.08	0.92	0.61	thf
bpz	0.05	–1.48 (78)	–2.36 (81)	–2.83	0.88	0.60	dmf

[a] From cyclic voltammetry or square-wave voltammetry at 298 K in 0.1 M solvent/Bu_4NPF_6 solutions. Scan rate: 100 mV s^{-1}. Potentials (E) in V vs. ferrocene/ferrocenium. Reduction potentials are given as half-wave potentials (E_1 or E_2), with peak-to-peak separation ΔE_{pp} in mV given in parentheses, or cathodic peak potentials (E_{R3}). Oxidation potentials are given as anodic peak potentials (E_{O1}).

Table 3. Electrochemical data of nickel complexes with Fmes or PPh_3 ligands.[a]

Compound	E (oxII)[b]	$E_{1/2}$ (oxI) (ΔE_{pp})[c]	$E_{1/2}$ (redI) (ΔE_{pp})[c]	$E_{1/2}$ (redII) (ΔE_{pp})[c]	Solvent/T [K]
[(bpy)Ni(Fmes)Br]	–	0.86 irr.[b]	–1.68 (66)	–2.13 (85)	thf/298
[(bpy)Ni(Fmes)Br]	1.89	0.92 irr.[b]	–	–	CH_2Cl_2/298
[(bpy)Ni(Fmes)Br]	1.90	0.81 (83)	–	–	CH_2Cl_2/258
$[(PPh_3)_2Ni(Mes)Br]$	1.62	0.58 irr.[b]	–2.55 irr.[d]	–	CH_2Cl_2/298
$[(PPh_3)_2Ni(Fmes)Br]$	1.66	0.85 (79)	–2.18 irr.[d]	–2.44 irr.[d]	CH_2Cl_2/298
$[(PPh_3)_2Ni(Fmes)Br]$	–	0.93 (76)	–1.99 irr.[d]	–2.92 irr.[d]	thf/298

[a] From cyclic voltammetry in 0.1 M solvent/Bu_4NPF_6 solutions at 100 mV s^{-1} scan rate. Potentials (E) in V vs. ferrocene/ferrocenium couple. [b] Anodic peak potentials (E_{pa}) for irreversible oxidation steps. [c] Half-wave potentials $E_{1/2}$, with peak potential differences $\Delta E_{pp} = E_{pa} - E_{pc}$ in mV in parentheses. [d] Cathodic peak potentials (E_{pa}) for irreversible reduction steps.

adequately reflected by the reduction potential. For the phosphane complexes $[(PPh_3)_2Ni(Mes)Br]$ and $[(PPh_3)_2Ni(Fmes)Br]$ the reductions occur at rather negative potentials and are irreversible even at low temperatures and in the presence of excess bromide.

For the diimine complexes [(N^N)Ni(Mes)Br] we can now draw a reaction scheme (Scheme 4) to illustrate the proposed EC mechanism as well as further feasible electrochemical or chemical reactions.

The first reduction (E_1) is followed by a rapid cleavage of bromide (C_1). The transient 15 VE species can be stabilised by coordinating a solvent molecule (C_2) or by dimerisation ($C_{2'}$). Coordinatively unsaturated species have been observed for other late transition metal complexes[29] but can be ruled out for our investigation since thf or dmf should have sufficient donor capacity to act as a ligand. The solvent complexes can be described by two different canonical forms $[(N\hat{}N^{\cdot-})Ni^{II}(Mes)(solv)] \leftrightarrow [(N\hat{}N)Ni^{I}(Mes)(solv)]$, which have either a reduced diimine ligand or monovalent nickel. The dimerisation occurs upon formation of a nickel–nickel bond with a formal Ni^{I}–Ni^{I} unit. Examples of this type of reaction have been found, for example, in the Ru^{I}–Ru^{I} dimers that are formed after electrochemical reduction of the Ru^{II} complexes $[(bpy)Ru(CO)_2X_2]$,[24] or in the formation of Re^0–Re^0 dimers $[(L)(CO)_3Re–Re(CO)_3(L)]$ from $[Re(CO)_3(L)X]$ (L = bpy or phen; X = Cl or CN).[26] Both are formal d^7–d^7 systems. Examples for related d^9–d^9 dimers are the Pd^{I}–Pd^{I} systems [(phen)(MeCN)Pd–Pd(MeCN)(phen)]$^{2+}$, formed from a comproportionation reaction of Pd^{II} and Pd^0 precursors,[30] and $[(L)(RNC)Pd–Pd(RNC)(L)]^{2+}$ (L = bpy, phen or dmphen; RNC = 2,4,6-$Me_3C_6H_2NC$).[31] A bpy-bridged Pt^{I}–Pt^{I} dimer is present in $[Pt_2(bpy)_3]^{2+}$, which is formed upon electroreduction of $[Pt(bpy)_2]^{2+}$.[32]

The E_{R2} and E_{R3} processes might thus correspond to the reduction of the solvent complexes or dimers, respectively. From the observation that the reduction wave E_{R2} is dominant in the case of the more basic ligands like bpy, whereas for the good acceptor ligands like bpz or bpm the second electron is accepted predominantly in the more negative

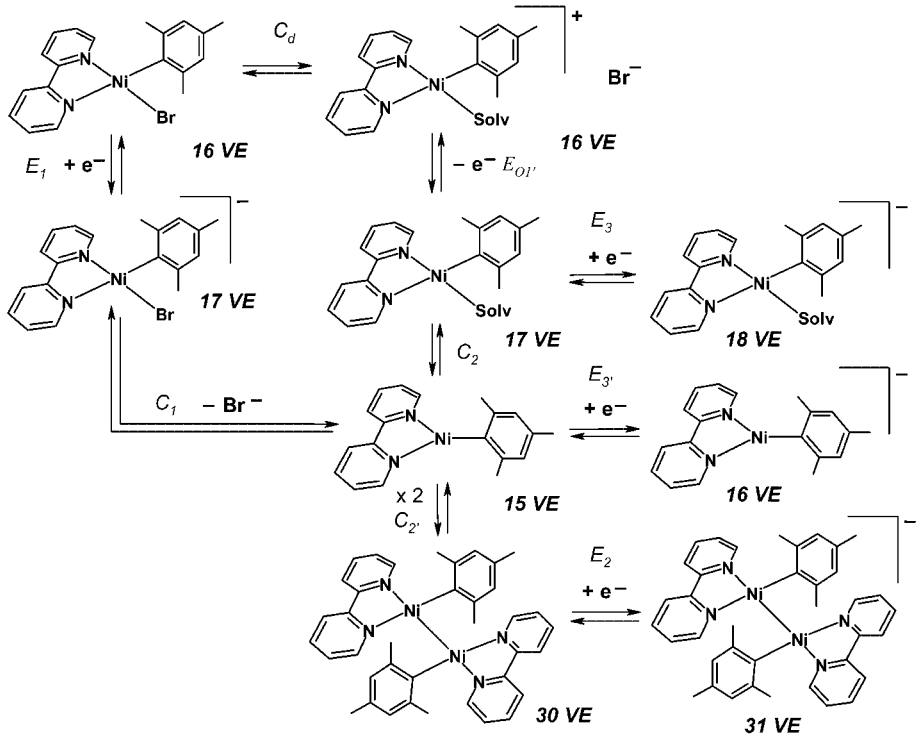

Scheme 4. Proposed mechanism for the electrochemical (E) and chemical reactions (C).

wave E_{R3}, we can assume a higher tendency of the complexes with basic diimine ligands to form dimeric species (30 VE) and a higher preference for the monomer radicals (17 VE) in the case of complexes with good acceptor ligands. Support for this assumption comes from the fact that using dmf instead of thf shifts the equilibrium between monomeric and dimeric species towards the monomeric solvent-stabilised species. At low temperatures the chemical processes are hampered and therefore we can partially observe the second reduction wave of the parent complexes $E_{R3'}$.

Oxidation Reactions

When measured at 298 K the nickel diimine complexes all exhibit irreversible oxidation waves (Tables 1, 2 and 3), which can be attributed to Ni^{II}/Ni^{III} couples. The potentials are quite low and vary according to the expected influence of the chelate ligand. For rather basic ligands like tmphen they occur at the least positive potentials. The bromido mesityl complexes generally show higher potentials than the dimesityl derivatives. The precursor complex $[(PPh_3)_2Ni(Mes)Br]$ exhibits a far higher potential than the corresponding diimine complexes and the Fmes co-ligand shifts the oxidation potentials to higher values. At lower temperatures the dimesitylnickel complexes exhibit some degree of reversibility for the first oxidation wave, which is in agreement with observations for related platinum(II)[33] or palladium(II)[34] complexes where sterically shielding mesityl ligands have allowed the observation of trivalent states. However, the latter exhibit reversible waves already at 298 K, whereas the nickel analogues are not fully reversible even at 213 K. The phosphane complex $[(PPh_3)_2Ni(Mes)Br]$ shows irreversible oxidation behaviour even at 213 K. A remarkable difference is observed for the oxidation waves of the Fmes derivatives. [(bpy)Ni(Fmes)Br] exhibits a fully reversible first oxidation at 243 K and $[(PPh_3)_2Ni(Fmes)Br]$ shows full reversibility at 298 K. Since a stabilisation of the trivalent nickel species for the non-fluorinated derivatives cannot be achieved even with two shielding mesityl groups, we assume that this enhancement is not only due to the better steric shielding by the CF_3 groups but also to the electron-withdrawing effect. Furthermore, we assume that C–H activation of the axial methyl groups plays an essential role in the decomposition of the corresponding mesityl derivatives. The superior stability of the CF_3 analogues might thus be due to the hampering of this pathway. Future investigations will therefore focus on the follow-up products of these oxidation reactions.

Bulk Reductive Electrolysis

To support the assumptions depicted in Scheme 4 we tried to isolate defined products from solutions of [(bpy)Ni(Mes)Br] in thf/Bu_4NPF_6 that had been submitted to bulk electrolysis (see Experimental Section). When the electrolysis was not driven to completeness, the main species isolated was the starting material together with the free bpy ligand as by-product. After exhaustive electrolysis mainly free bpy ligand and traces of the dimesityl complex [(bpy)Ni(Mes)$_2$] were found, as already mentioned above.

Spectroelectrochemistry

In order to support the above assignments we studied the products of the electrochemical or chemical reactions by controlled electrolyses combined with in situ spectroscopy (UV/Vis/NIR or EPR).

Reductive UV/Vis/NIR Spectroelectrochemistry

Optical spectroscopy was used to study the products generated in situ from the reductive electrochemistry as this should allow us to answer the question whether the chelate ligand or the metal is hosting the odd electron in the reduced species and furthermore help to discriminate between the formation of solvent complexes [(N^N)Ni(Mes)(solv)] or dimers [(N^N)(Mes)Ni–Ni(Mes)(N^N)] and allow us to characterise them. Figures 4, 5 and 6 show some representative spectra, and Tables 4 and 5 summarise the obtained data.

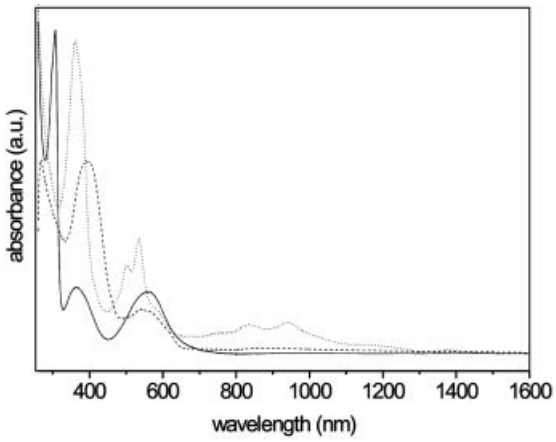

Figure 4. Absorption spectra of $[(bpy)Ni(Mes)_2]^n$ (n = 0: solid line; –1: dotted; –2: dashed) from UV/Vis/NIR spectroelectrochemistry in dmf/Bu_4NPF_6 solution. Note that in the last spectrum there is some residual absorption around 900 nm, which is due to an incomplete second reduction.

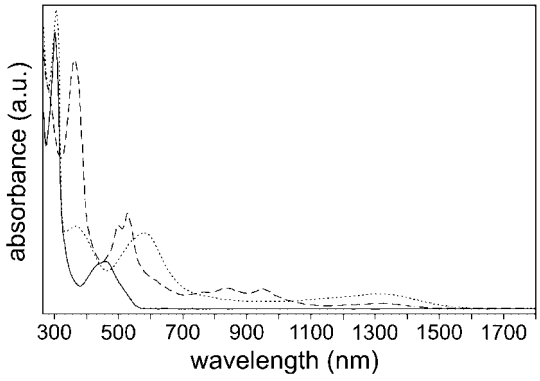

Figure 5. UV/Vis/NIR spectroelectrochemistry of [(bpy)Ni(Mes)Br] in dmf/Bu_4NPF_6 solution. Absorption spectra of the parent compound (solid) and after one-electron reduction, spectrum at higher concentration (about 5×10^{-2} M, dotted) and dilute solution (about 10^{-4} M, dashed).

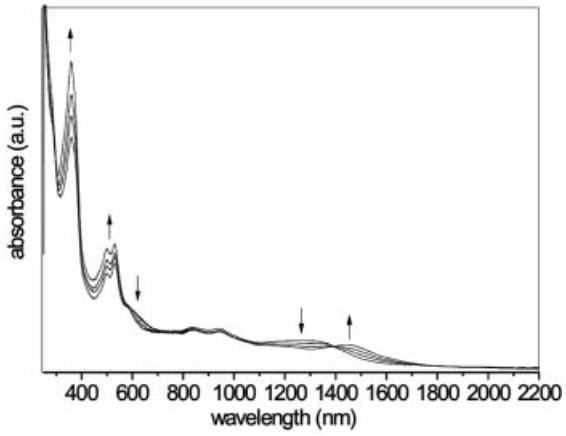

Figure 6. UV/Vis/NIR absorption spectra of [(bpy)Ni(Mes)Br] during the second reduction in dmf/Bu_4NPF_6 solution.

Table 4. Long-wavelength absorption maxima of reduced nickel complexes $[(N^{\wedge}N)Ni(Mes)_2]^{n-}$ (N^N = bpy, bpz or tmphen).[a]

	λ_1 (ε)	λ_2 (ε)	λ_3 (ε)	λ_4 (ε)	λ_5 (ε)
bpy/n = 0	298 (15.1)	367 (3.2)	564 (3.1)	–	–
n = 1	–	355 (14.9)	530 (6.0)	940 (1.7)	–
n = 2	–	–	392 (7.4)	530 (2.6)	–
bpz/n = 0	–	394 sh	632	–	–
n = 1	449 sh	493 sh	642	1055	1200
n = 2	355	493	589 sh	1070 sh	1258
tmphen/n = 0	278	341 sh	521	–	–
n = 1	345 sh	369 sh	534	617 sh	820 sh
n = 2	381	489	604	843	962

[a] Generated and measured in dmf/Bu_4NPF_6 solution, absorption maxima in nm with extinction coefficients ε ($\times 1000\ M^{-1}cm^{-1}$) in parentheses.

Figure 4 shows the optical spectra of $[(bpy)Ni(Mes)_2]$ in the parent, singly reduced and doubly reduced state. The long-wavelength absorption bands of the reduced species can be assigned to intra-ligand transition from the singly (or doubly) occupied former LUMO,[23,31] which has been calculated recently to be 96% centred on the bpy ligand,[21] thus clearly showing the mainly bpy-centred character of the reductions. The same assignments can be made for the bpz and tmphen derivatives (see Table 4).

When performing the same spectroelectrochemical experiment for the bromido mesityl derivative (Figure 5 and Table 5) we found that the observed absorption bands of the one-electron-reduced complex were concentration dependent. At high concentrations (about 5×10^{-2} M) the spectrum is characterised by a weak broad long-wavelength band around 1300 nm, two medium strong bands around 600 and 350 nm and a very strong band at 300 nm. In dilute solutions ($<10^{-4}$ M) two structured band systems around 900 and 500 nm are visible together with a UV band at around 350 nm. At 1300 nm there is only a very weak residual absorption. Medium concentrated solutions show all the above-described band systems simultaneously. In view of the dimesityl system (Figure 4) and the corresponding spectra of the free ligands,[35] we can ascribe the spectral features of dilute solutions to a species containing a reduced bipyridine ligand and we assume this to be the radical complex $[(bpy^{-})Ni(Mes)(solv)]^{\cdot}$. Apart from the 1300-nm band, the spectra of concentrated solutions resemble those of the starting complex. We tentatively assign this species to the dimer [(bpy)(Mes)Ni–Ni(Mes)(bpy)] since the observed species does not seem to contain a reduced bpy ligand. The 1300-nm band might be ascribed to a transition arising from the nickel–nickel bond (probably a σ–σ* transition).

Table 5. Long-wavelength absorption maxima of parent complexes and species resulting from reductive electrolysis of bromido mesityl complexes [(N^N)Ni(Mes)Br] + n electrons.[a]

(N^N) n	Species	λ (ε)			
tmphen					
n = 0	parent	281	409	–	–
n = 1	dimer	285, 345	516	637 sh	–
n = 2	dimer	292	385, 490, 608	852, 921	–
dmbpy					
n = 0	parent	301	439, 470	–	–
n = 1	monomer	363	518, 550	788	–
n = 1	dimer	300	524	779	1410
n = 2	dimer	352	352, 512, 527	794	1512
bpy					
n = 0	parent	308 (17.2)	465 (2.3)	–	–
n = 1	monomer	361 (14)	500 (5.0), 532 (5.4)	945 (1.2)	–
n = 1	dimer	310 (17.8)	370 (4.5)	580 (4.4)	1305 (1.0)
n = 2	dimer	372 (15.5)	500 (6.1), 530 (6.3)	942 (1.3)	1448 (1.0)
bpz					
n = 0	parent	325	538	–	–
n = 1	monomer	333, 382	530	1092	–
n = 2	monomer	344, 385	780	–	–
bpm					
n = 0	parent	275	340 sh, 530	–	–
n = 1	monomer	355	460, 482	635	–
n = 2	monomer	345	585	–	–

[a] Generated and measured in dmf/Bu_4NPF_6 solution, absorption maxima in nm with the extinction coefficients ε ($\times 1000\ M^{-1}cm^{-1}$) in parentheses.

Furthermore, the spectra exhibit two broad medium-strong bands in the visible and a strong band in the UV region. From comparison with the mononuclear dimesityl and bromido mesityl complexes[21] the first two are assigned to mixed MLCT/L′LCT and the latter to π–π* transitions. Careful inspection of the depicted spectra reveals that all spectra exhibit both of the species in varying amounts, which is in line with the assumed equilibrium in Scheme 4. Comparison of all the studied systems (Table 5) shows that after one-electron reduction the spectra of complexes with more basic diimine ligands preferably show the broad band systems indicative for dimeric species. In the extreme case of the tmphen derivative we assign the spectral features to solely the dimeric species. In contrast to this, for the good π-acceptor ligands bpz or bpm no dimer formation is observed, and instead only the monomeric radical complexes are detected (several structured band systems). Furthermore, in systems where both monomeric and dimeric species are observed we found an influence of the solvent on the equilibrium. In thf solution a higher tendency to form dimeric species is observed, whereas in dmf the monomeric radicals (solvent stabilised) are favoured; this is due to the better donor behaviour of the latter solvent.

Figure 6 shows the addition of a second electron to a solution of [(bpy)Ni(Mes)Br] in dmf. We assume that the starting spectrum represents a mixture of the mononuclear species [(bpy^{-})Ni(Mes)Br]$^{\bullet}$ and the dimer [(bpy)(Mes)Ni–Ni(Mes)(bpy)]. At the potential applied behind the peak E_{R2} the dimer is reduced to form the radical [(bpy^{-})(Mes)-Ni–Ni(Mes)(bpy)]$^{\bullet-}$ whereas the monomeric species does not undergo any change. This consideration is based on the red-shift of the long-wavelength band and the increase of the structured band systems around 500 and 350 nm. The two latter bands are indicative of a mono-reduced bipyridine ligand (in the dimeric complex); no evidence is found for a doubly reduced ligand.

For the good π-acceptor ligands bpz and bpm all spectral features clearly represent the reduced ligand and no long-wavelength band indicative of the dimer formation can be detected. Therefore, we assign the two observed reduction processes to the sequence E_1–C_1–C_2–E_3.

Oxidative UV/Vis/NIR Spectroelectrochemistry

Oxidation of the diimine nickel(II) complexes [(N^N)-Ni(Mes)Br] or [(N^N)Ni(Mes)$_2$] leads to rapid decomposition of the complexes at 298 K under the conditions of our spectroelectrochemical experiments, therefore we cannot present any spectroscopic data for the generated trivalent species. Spectroelectrochemical experiments at low temperature might help but are not possible for us at present.

EPR Spectroelectrochemistry

Since many of the proposed species are radicals, EPR spectroscopy should give some evidence for the proposed mechanisms for the reductive electrochemistry. EPR data can also provide conclusive information on the metal or ligand contribution to the singly occupied molecular orbital (SOMO)[20] for species from both reductive and oxidative electrochemistry.

Reductive EPR Spectroelectrochemistry

The EPR spectra of the anion radicals of the dimesitylnickel complexes [(N^N)Ni(Mes)$_2$]$^{\bullet-}$ all exhibit relatively narrow resonances with hyperfine splitting (HFS) in the range of 0.1–0.5 mT. Such HFS constants are typical for couplings of the unpaired electron to the protons and nitrogen atoms of the diimine ligand. Together with the *g* values, which are close to the free-electron value of 2.0023, this is a strong indication for an almost pure π*(diimine) character of the singly occupied molecular orbital (SOMO). For bpy a simulation of the spectrum gave 0.335 mT for N, 0.408 mT for H5, 0.150 mT for H3, 0.081 mT for H4 and 0.065 mT for H6.[23]

At low temperatures in glassy frozen solutions a rhombic-type spectrum was obtained for [(bpy)Ni(Mes)$_2$]$^{\bullet-}$ with g_1 = 2.014, g_2 = 2.004 and g_3 = 1.996. The averaged value is in agreement with g_{iso} = 2.0049. The small *g* anisotropy (Δg = 0.018) is indicative of a quite small metal contribution to the radical anion, in agreement with the g_{iso} and the HFS signal found at 298 K. Therefore, and in agreement with the findings from UV/Vis/NIR spectroelectrochemistry and from previous studies on the frontier orbitals of these complexes,[21] we can conclude that the first reduction of the dimesityl complexes occurs into orbitals with mainly π*(diimine) character. Very similar spectra were obtained for the tmphen and bpz derivatives (Table 6). The corresponding radicals are best described as reduced diimine ligands bound to a nickel(II) centre [(N^N^{-})Ni^{II}(Mes)$_2$]$^{\bullet-}$.

The first signal observed during reductive electrolysis of [(bpy)Ni(Mes)Br] in thf/Bu_4NPF_6 solution at the first reduction wave is rather narrow, shows partial HFS and has a *g* value of 2.0016 (Figure 7, top). Electrolysis at more negative potential (second wave) first leads to an increase of the intensity of this signal and, after a few minutes, an additional, comparably broad signal appears (Figure 7, bottom left) which lies at far higher *g* (2.140) and does not show any HFS. Measurements of this solution at 110 K (glassy frozen solution) reveal that the high-*g* species now exhibits a rhombic-type spectrum, whereas the low-*g* species remains isotropic and narrow (Figure 8).

Table 6. EPR data from reductive spectroelectrochemistry of dimesitylnickel complexes.[a]

Complex	*T* [K]	g_{iso}/g_{av}	g_1	g_2	g_3	Δg [b]	ΔH [c] [mT]
[(tmphen)Ni(Mes)$_2$]$^{\bullet-}$	298	2.0067					2.8
[(bpy)Ni(Mes)$_2$]$^{\bullet-}$	298	2.0049					3.1
[(bpy)Ni(Mes)$_2$]$^{\bullet-}$	110	2.0047	2.014	2.004	1.996	0.018	–
[(bpz)Ni(Mes)$_2$]$^{\bullet-}$	298	2.0063					4.0

[a] Generated and measured in thf/Bu_4NPF_6 solution. [b] *g* anisotropy $\Delta g = g_1 - g_3$. [c] Signal width.

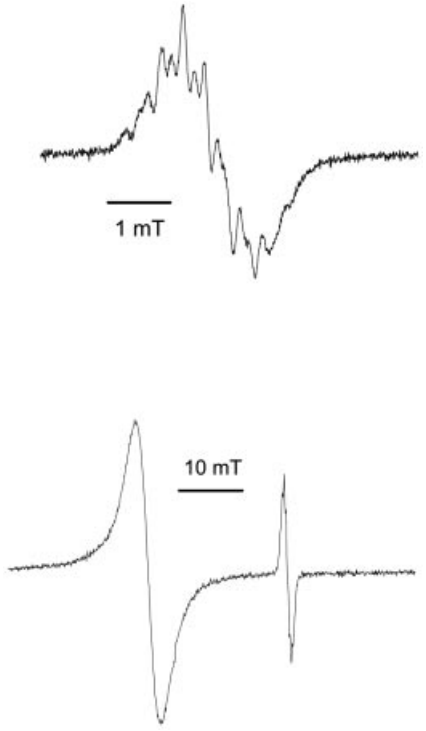

Figure 7. EPR spectra obtained during electrochemical reduction of [(bpy)Ni(Mes)Br] in thf/Bu_4NPF_6 at 298 K. Signals obtained upon first (top) and second reduction (bottom).

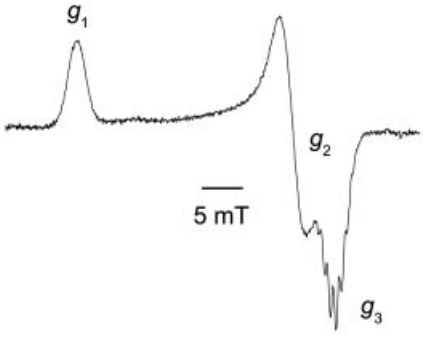

Figure 8. EPR spectrum of a solution obtained at the second reduction wave of [(bpy)Ni(Mes)Br] in thf/Bu_4NPF_6, measured at 110 K (glassy frozen solution). The isotropic spectrum (with HFS) of the monomeric complex is overlapping with the g_3 component of the main signal (see text and Table 7).

No signal was observed for tmphen at 298 K, although freezing the electrolysed solutions to 110 K allowed the observation of an unresolved narrow signal at $g = 1.9999$ that is comparable to the low-g signal of the bpy derivative. For bpym, bpz, bpm and *i*Pr-DAB we obtained narrow signals with HFS and g values of about 2. For the bpm derivative the solution frozen at 110 K yielded an axial signal with very small g anisotropy. Summarising the data collected in Table 7 we can make the following assignments and conclusions. The signals with g values around the value of the free electron (2.0023) and with detectable HFS were assigned to monomeric nickel(II) complexes containing reduced diimine ligands $[(N\text{^}N^{-})Ni^{II}(Mes)L]^{\cdot}$ (L = Br or solvent). These are the only signals obtained for most of the complexes, which is in line with the observation from UV/Vis/NIR absorption spectroscopy for the good acceptor ligands (vide supra). A second signal was observed for bpy after the reduction at more negative potential, with no HFS, a far higher isotropic g value and a rather high g anisotropy. The two latter parameters point to a far higher nickel contribution to the unpaired electron in this species, which is in line with the assumption that the corresponding species is the proposed dimer in its reduced state $[(bpy^{-})(Mes)Ni^{I}–Ni^{I}(Mes)(bpy)]^{\cdot-}$. For tmphen the observation of such dimeric species would be also expected from the trend of monomer–dimer equilibrium discussed in the electrochemistry section. So far we do not understand the reason why we did not observe any signal at 298 K. At low temperatures we observed only a narrow signal indicative of a monomeric radical.

It is also noteworthy that the EPR results did not give any evidence for the corresponding radicals $[(N\text{^}N^{-})Ni^{II}(Mes)_2]^{\cdot-}$. This confirms our conclusion from the electrochemistry that no large amounts of the dimesityl complexes are formed during reductive electrolysis on the first two reduction waves.

Oxidative EPR Spectroelectrochemistry

As outlined above the UV/Vis/NIR spectroelectrochemical experiments did not allow the observation of nickel(III) species due to rapid decomposition at 298 K. Since the spectroelectrochemical cell used for EPR studies allows electrolysis at lower temperature we tried to study the oxi-

Table 7. EPR data from species observed during reductive spectroelectrochemistry of bromido(mesityl)nickel complexes [(N^N)Ni(Mes)Br].[a]

(N^N)	Proposed species	Solvent	T [K]	g_{iso}/g_{av}	g_1	g_2	g_3	Δg[b]	ΔH[c] [mT]
tmphen	monomer	dmf	110	1.9999					8.0
bpy	monomer	thf	298	2.0016					3.1
	dimer	thf	298	2.140					15.0
	dimer	thf	110	2.139	2.214	2.198	2.007	0.207	–
	dimer	dmf	110	2.1311	2.2635	2.0785	2.0449	0.2186	–
bpym	monomer	thf	298	2.0038					3.0
	monomer	dmf	298	2.0038					3.0
bpz	monomer	thf	298	2.0112					3.8
bpm	monomer	thf	298	2.0039					3.2
	monomer	thf	110	1.9969	2.0024	2.0024	1.9854	0.0165	–
*i*Pr-DAB	monomer	thf	298	2.0038					3.0

[a] Generated and measured in solvent/Bu_4NPF_6 solutions. [b] g anisotropy $\Delta g = g_1 - g_3$. [c] Signal width.

dation process of selected nickel(II) complexes and the generated nickel(III) species by EPR spectroscopy. Although we examined a number of compounds, only the complex *trans*-[$(PPh_3)_2$Ni(Fmes)Br] gave a reasonable EPR signal (Figure 9). This is not unexpected in view of its promising reversible cyclic voltammetric behaviour (Table 3).

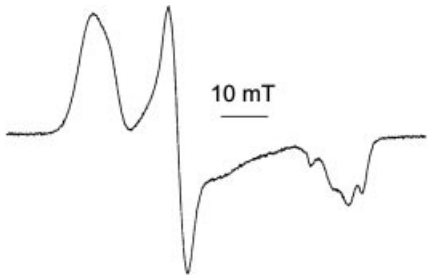

Figure 9. X-band EPR spectrum obtained during electrochemical oxidation of *trans*-[$(PPh_3)_2$Ni(Fmes)Br] in CH_2Cl_2/Bu_4NPF_6 at 258 K. Measured at 4 K in a glassy frozen solution.

No signal was observed at the corresponding electrolysis temperature of 258 K. At 4 K a rhombic signal (Figure 9) was obtained with very large anisotropy and high averaged g value (g_1 = 2.825, g_2 = 2.453, g_3 = 1.947, Δg = 0.878, $g_{av.}$ = 2.435). The g_3 component shows a partial HFS of about 5–6 mT and g_1 also shows some signs of HFS, whereas the g_2 component is sharp and unstructured. In view of the rather high g anisotropy we assign this signal to a radical with a very high nickel contribution to the unpaired electron, and thus to a "real" nickel(III) complex [$(PPh_3)_2Ni^{III}$(Fmes)Br]$^{\cdot+}$ with square-planar geometry, a d^7 low-spin configuration and S = 1/2 spin state. There are only very few comparable monomolecular organonickel(III) species reported so far. EPR measurements at low-temperature for the homoleptic complex [$Ni(C_6Cl_5)_4$]$^{\cdot-}$ gave an axial signal with $g_\perp$ = 2.84, $g_\parallel$ = 1.92 and a g anisotropy of 0.92,[36] which is comparable to the value found for our species. For the arylnickel(III) species [(*NCN*)$NiCl_2$], which contains a bis(dimethylamino)phenyl pincer ligand, a g anisotropy of 0.345 has been found.[37] For non-organometallic, formally nickel(III) species the g anisotropy is usually much lower, for example Δg = 0.486 for [Ni(emi)]$^-$ [H_4emi = *N*,*N*-ethylenebis(2-mercaptoisobutyramide)],[38] Δg = 0.372 for the related tetramidonickel complex [Ni(L)]$^{\cdot-}$ (H_4L = 6,6-diethyl-3,3,9,9,12,12,14,14-octamethyl-1,4,8,11-tetraazacyclotetradecane-2,5,7,10,13-pentaone; see Scheme 5),[39] or Δg = 0.247 for the oxamato complex [Ni(L′)]$^{\cdot-}$ (H_4L′ = *N*-[2-(oxalylamino)phenyl]oxalamic acid).[40] Whereas for many species formally described as nickel(III) an appropriate ligand contribution to the unpaired electron from non-innocent ligands such as imines, oxamates or thiolates must be assumed, the [Ni(L)]$^{\cdot-}$ system contains an innocent tetramido ligand, thus an almost pure metal-centred SOMO can be supposed.[39] Comparing its g anisotropy with the values obtained for the two organonickel systems discussed above, it seems that organo ligands lead to distinctly higher g anisotropy and thus highly metal-centred radical states. However, the very small number of examples allows only very tentative conclusions and it would be worthwhile to synthesise further examples of trivalent organonickel complexes.

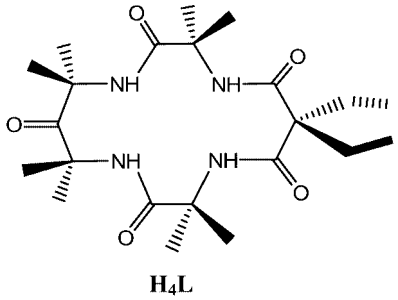

H_4L

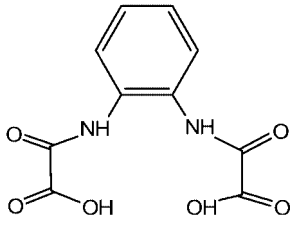

H_4L'

Scheme 5. Drawings of macrocyclic ligands H_4L and H_4L′.

Conclusions

Electrochemical reduction of the organometallic nickel(II) complexes [(N^N)Ni(Mes)Br] leads to highly reactive radicals which undergo follow-up chemical reactions. The nature of the products could not be established unambiguously, but strong evidence was found from optical and EPR spectroelectrochemistry that radical solvent complexes [(N^N)NiMes(Solv)]$^{\cdot}$ with a mainly diimine ligand centred SOMO are formed in processes that start with a ligand-centred one-electron reduction, followed by a splitting of the bromide ligand (EC process). Strong evidence for this comes from various electrochemical experiments and comparison with UV/Vis/NIR absorption and EPR spectra of the corresponding dimesityl radical complexes [(N^N)-$Ni(Mes)_2$]$^{\cdot-}$. For both dimesityl and bromido mesityl complexes a description as monovalent nickel species is not appropriate.

In the case of the comparably basic ligands tmphen, dmbpy or bpy additional spectroscopic features were assigned to the formation of dimers [(N^N)(Mes)Ni–Ni-(Mes)(N^N)] with monovalent nickel after the splitting of the bromide ligand. Evidence comes from long-wavelength bands in the corresponding UV/Vis/NIR spectra and from the EPR signals of the corresponding reduced species at more negative potentials (second reduction) with comparably high g values and g anisotropy in the solid state. Unfortunately, attempts to isolate the proposed dimer complexes using preparative electrochemical reduction (bulk electrolysis) have failed so far, which is a pity in view of catalytic applications.

Oxidation of the nickel(II) complexes leads to very short-lived trivalent nickel species that have been characterised by EPR spectroscopy for the perfluorinated complex $[(PPh_3)_2Ni(Fmes)Br]^{\cdot+}$. An almost pure metal-centred character for the SOMO can be concluded from the very high *g* anisotropy of the rhombic signal obtained at 4 K.

Thus, we can add some new evidence to the proposed mechanism for the electrochemical C–C coupling reactions catalysed by nickel diimine complexes. The mechanism has so far been explored in detail up to the catalytically active species [(N^N)Ni(aryl)X]. We can conclude from our work that: i) the assumption of nickel(I) species after the first electrochemical reduction must be corrected towards a mainly diimine ligand centred reduction. Nevertheless, the splitting of the bromide occurs very rapidly, regardless of the character of the SOMO; ii) the diaryl complexes $[(N^N)Ni(aryl)_2]$ are formed in only very small quantities from decomposed material during reductive electrolysis; the formation of nickel(I)–nickel(I) dimers [(N^N)(aryl)Ni–Ni(aryl)(N^N)], which might have an impact on the catalysis, seems to be more important; iii) the proposed monomeric nickel(III) species after oxidative addition of aryl halides have gained some evidence as plausible transient states from our investigations. It seems that organo ligands favour nickel-centred radical states; although this has been demonstrated for a complex containing phosphane instead of diimine ligands. The trivalent diimine nickel species generated upon one-electron oxidation of [(N^N)Ni(Mes)(L)] (L = Mes or Br] are highly unstable even at low temperatures and could not be detected by us.

Experimental Section

Instrumentation: ^{1}H NMR spectra were recorded with Bruker Avance300 or AC250 spectrometers. UV/Vis/NIR absorption spectra were recorded with a Bruins Instruments Omega 10 photospectrometer. Cyclic voltammetry and square-wave voltammetry were carried out in 0.1 M Bu_4NPF_6 solutions using a three-electrode configuration (glassy-carbon working electrode, Pt counter electrode, Ag/AgCl reference) and a PAR 273 potentiostat and function generator. Half-wave ($E_{1/2}$), anionic (E_{pa}) or cationic peak potentials (E_{pc}) are given with respect to the ferrocene/ferrocenium couple, which also serves as internal reference. Polarographic measurements were carried out with a PAR Model 263A device. EPR spectra at X-band frequency (ca. 9.5 GHz) were obtained with a Bruker ESP300 spectrometer equipped with a Bruker ER035M gaussmeter and a HP 5350B microwave counter. Spectral simulations were performed with Bruker SimFonia V1.25. UV/Vis/NIR spectroelectrochemical measurements were performed with an optically transparent thin-layer electrode (OTTLE) cell.[41] EPR spectroelectrochemical studies were performed with a platinum two-electrode cell.

Materials and Procedures: The preparation of the complex $[(PPh_3)_2Ni(Mes)Br]$ and the diimine complexes [(N^N)Ni(Mes)Br] and $[(N^N)Ni(Mes)_2]$ has been reported recently.[21–23] All preparations and physical measurements in this work were carried out in dry solvents under argon, using Schlenk techniques.

Preparation of *trans*-[$(PPh_3)_2$Ni(Fmes)Br]: $NiBr_2$ (218 mg, 1 mmol) was suspended in 200 mL of thf. After addition of PPh_3 (524 mg, 2 mmol) the solution turned green. After refluxing for 2 h the reaction mixture was cooled to 298 K and Li(Fmes) (374 mg, 1.3 mmol) in 100 mL of diethyl ether was added. The mixture was stirred for 18 h then 10 mL of aqueous saturated NH_4Cl solution was slowly added to give orange precipitate in the aqueous phase. After separation of the phases and washing the aqueous phase with three 10-mL portions of thf the combined thf solutions were dried with anhydrous Na_2SO_4 (1 h) then filtered and the solvents evaporated to dryness. The resulting orange material was recrystallised twice from thf to give red crystals. Yield: 651 mg (0.69 mmol, 69%). $C_{45}H_{32}BrF_9NiP_2$ (944.30): calcd. C 57.24, H 3.42; found C 57.28, H 3.46. ^{1}H NMR ([D$_6$]acetone): δ = 7.9–7.3 (m, 30 H, Ph–P), 7.03 (s, 2 H, Fmes) ppm. ^{1}H NMR ($CDCl_3$): δ = 8.2–7.1 (m, 30 H, Ph–P), 6.93 (s, 2 H, Fmes) ppm. ^{13}C NMR ([D$_6$]acetone): δ = 137.1 (C^1–P), 136.4 (C^1Fmes), 133.6 ($C^{2,6}$P), 131.5 (C^4Fmes), 131.0 ($C^{2,6}$Fmes), 128.6 (C^4–P), 128.4 ($C^{3,5}$–P), 125.0 ($C^{3,5}$Fmes) ppm. ^{31}P NMR ($CDCl_3$): δ = 15.55 ppm (s). ^{19}F NMR ($CDCl_3$): δ = –56.59 (t, $^5J_{P,F}$ = 5.9 Hz, 3 F, *o*-CF_3), –63.13 (s, 3 F, *p*-CF_3) ppm.

Preparation of [(bpy)Ni(Fmes)Br]: The compound was prepared by stirring a solution of *trans*-[$(PPh_3)_2$Ni(Fmes)Br] (110 mg, 0.116 mmol) together with bpy (28 mg, 0.18 mmol) in diethyl ether overnight. After evaporation to dryness, the resulting orange-brown solid was washed with *n*-heptane to remove the PPh_3 and excess bpy. It was then recrystallised from acetone to give orange needles. Yield: 57 mg (0.1 mmol, 85%). $C_{19}H_{10}BrF_9N_2Ni$ (575.91): calcd. C 39.63, H 1.75, N 4.87; found C 39.61, H 1.78, N 4.88. ^{1}H NMR ([D$_6$]acetone): δ = 9.07 (d, $^3J_{6,5}$ = 5.62 Hz, 2 H, bpy-H6), 8.42 (d, $^3J_{3,4}$ = 8.1 Hz, 2 H, bpy-H3), 8.40 (d, $^3J_{3',4'}$ = 7.86 Hz, 2 H, bpy-H3′), 8.28 (dd, $^3J_{4,5}$ = 6.23 Hz, 2 H, bpy-H4), 8.25 (dd, $^3J_{4',5'}$ = 5.62 Hz, 2 H, bpy-H4′), 7.80 (s, 2 H, Fmes), 7.75 (ddd, 2 H, bpy-H5), 7.40 (ddd, $^3J_{6',5'}$ = 5.72 Hz, 2 H, bpy-H5′), 7.18 (d, 2 H, bpy-H6′) ppm. ^{19}F NMR ([D$_6$]acetone): δ = –58.1 (s, 6 F, *o*-CF_3), –62.97 (s, 3 F, *p*-CF_3) ppm.

Bulk Reductive Electrolysis: Electrolysis experiments were carried out with solutions of [(bpy)Ni(Mes)Br] in thf/Bu_4NPF_6 using a Pt grid working electrode (total surface are of about 10 cm^2), a Pt counter electrode in a separate compartment (separated by a G4 glass frit) and an Ag/AgCl reference electrode. A PAR 273 potentiostat and function generator served to perform the electrolysis and allowed the control of electrons passed into the solution. Cyclic voltammograms were taken from time to time during the electrolysis and after electrolysis the solutions were evaporated to dryness. ^{1}H NMR spectra were either recorded for [D$_6$]acetone solutions of the obtained residues or recrystallised material (from thf/diethyl ether, 1:5).

Acknowledgments

This work was supported by the Grant Agency of the Academy of Sciences of the Czech Republic (grant no. A400400505).

[1] *Applied Homogeneous Catalysis with Organometallic Compounds* (Eds.: B. Cornils, W. A. Herrmann), Wiley/VCH, Weinheim, 2nd edition, **2002**.
[2] a) S. D. Ittel, L. K. Johnson, M. Brookhart, *Chem. Rev.* **2000**, *100*, 1169–1203; b) A. Michalak, T. Ziegler, *Organometallics* **2001**, *20*, 1521–1532; c) S. Mecking, *Angew. Chem. Int. Ed.* **2001**, *40*, 534–540; d) V. C. Gibson, S. K. Spitzmesser, *Chem. Rev.* **2003**, *103*, 283–315.
[3] J.-Y. Nédélec, J. Périchon, M. Troupel, *Top. Curr. Chem.* **1997**, *185*, 141–173.
[4] a) K. W. R. de Franca, J. de Lira Oliveira, T. Florencio, A. P. Da Silva, M. Navarro, E. Léonel, J.-Y. Nédélec, *J. Org. Chem.*

2005, *70*, 10778–10781; b) M. Durandetti, J. Périchon, *Synthesis* **2004**, 3079–3083; c) F. Raynal, R. Barhdadi, J. Périchon, A. Savall, M. Troupel, *Adv. Synth. Catal.* **2002**, *344*, 45–49; d) K. W. R. de Franca, M. Navarro, E. Léonel, M. Durandetti, J.-Y. Nédélec, *J. Org. Chem.* **2002**, *67*, 1838–1842.
[5] a) D. G. Yakhvarov, Y. H. Budnikova, O. G. Sinyashin, *Russ. J. Electrochem.* **2003**, *39*, 1261–1269; b) Y. H. Budnikova, Y. M. Kargin, J.-Y. Nédélec, J. Périchon, *J. Organomet. Chem.* **1999**, *575*, 63–66.
[6] C. Amatore, A. Jutand, J. Périchon, Y. Rollin, *Monatsh. Chem.* **2000**, *131*, 1293–1304.
[7] a) C. Gosmini, J.-Y. Nédélec, J. Périchon, *Tetrahedron Lett.* **2000**, *41*, 5039–5042; b) dito, *Tetrahedron Lett.* **2000**, *41*, 201–203; c) G. Meyer, M. Troupel, J. Périchon, *J. Organomet. Chem.* **1990**, *393*, 137–142.
[8] a) A. P. Da Silva, S. D. C. Mota, L. W. Bieber, M. Navarro, *Tetrahedron* **2006**, *62*, 5435–5440; b) A. P. Da Silva, A. C. S. Maia, M. Navarro, *Tetrahedron Lett.* **2005**, *46*, 3233–3235.
[9] D. M. Goken, D. G. Peters, J. A. Karty, J. P. Reilly, *J. Electroanal. Chem.* **2004**, *564*, 123–132.
[10] a) D. Franco, K. Wenger, S. Antonczak, D. Cabrol-Bass, E. Dunach, M. Rocamora, M. Gomez, G. Muller, *Chem. Eur. J.* **2002**, *8*, 664–672; b) S. Olivero, D. Franco, J.-C. Clinet, E. Dunach, *Collect. Czech. Chem. Commun.* **2000**, *65*, 844–861.
[11] C. Kuang, Q. Yang, H. Senbuko, M. Tokuda, *Chem. Lett.* **2005**, *34*, 528–529.
[12] P. Tascedda, E. Dunach, *Chem. Commun.* **2000**, 449–450.
[13] M. Ocafrain, E. Dolhem, J.-Y. Nédélec, M. Troupel, *J. Organomet. Chem.* **1998**, *571*, 37–42.
[14] S. Sengmany, E. Léonel, J. P. Paugam, J.-Y. Nédélec, *Tetrahedron* **2002**, *58*, 271–277.
[15] C. Amatore, A. Jutand, *Organometallics* **1988**, *7*, 2203–2214.
[16] D. G. Yakhvarov, Y. H. Budnikova, O. G. Sinyashin, *Russ. Chem. Bull. Int. Ed.* **2003**, *52*, 567–569.
[17] M. Durandetti, M. Devaud, J. Périchon, *New J. Chem.* **1996**, *20*, 659–667.
[18] D. G. Yakhvarov, D. I. Tazeev, O. G. Sinyashin, G. Giambastiani, C. Bianchini, A. M. Segarra, P. Lönnecke, E. Hey-Hawkins, *Polyhedron* **2006**, *25*, 1607–1612.
[19] a) D. G. Yakhvarov, E. G. Samieva, D. I. Tazeev, Y. H. Budnikova, *Russ. Chem. Bull. Int. Ed.* **2002**, *51*, 796–804; b) Y. H. Budnikova, J. Périchon, D. G. Yakhvarov, Y. M. Kargin, O. G. Sinyashin, *J. Organomet. Chem.* **2001**, *630*, 185–192.
[20] a) E. Alessio, S. Daff, M. Elliot, E. Iengo, L. A. Jack, K. G. Macnamara, J. M. Pratt, L. J. Yellowlees, *Spectroelectrochemical Techniques*, in *Trends in Molecular Electrochemistry* (Eds.: A. J. L. Pombeiro, C. Amatore), FontisMedia S. A., Lausanne, **2004**, p. 339–381; b) W. Kaim, *From Electron Transfer to Chemistry: Electrochemical Analysis of Organometallic Reaction Centers and of Their Interaction Across Ligand Bridges*, in *Trends in Molecular Electrochemistry* (Eds.: A. J. L. Pombeiro, C. Amatore), FontisMedia S. A., Lausanne, **2004**, p. 127–151; c) J. A. McCleverty, M. D. Ward, *Mono- and Dinuclear Molybdenum and Tungsten Complexes: Electrochemistry, Optics and Magnetics*, in *Trends in Molecular Electrochemistry* (Eds.: A. J. L. Pombeiro, C. Amatore), FontisMedia S. A., Lausanne, **2004**, p. 71–96.
[21] A. Klein, M. P. Feth, H. Bertagnolli, S. Záliš, *Eur. J. Inorg. Chem.* **2004**, 2784–2796.
[22] M. P. Feth, A. Klein, H. Bertagnolli, *Eur. J. Inorg. Chem.* **2003**, 839–852.
[23] A. Klein, *Z. Anorg. Allg. Chem.* **2001**, *627*, 645–650.
[24] a) S. Chardon-Noblat, A. Deronzier, R. Ziessel, *Collect. Czech. Chem. Commun.* **2001**, *66*, 207–227; b) S. Chardon-Noblat, A. Deronzier, F. Hartl, J. van Slageren, T. Mahabiersing, *Eur. J. Inorg. Chem.* **2001**, 613–617; c) S. Chardon-Noblat, G. H. Cripps, A. Deronzier, J. S. Field, S. Gouws, R. Haines, F. Southway, *Organometallics* **2001**, *20*, 1668–1675; d) S. Chardon-Noblat, A. Deronzier, R. Ziessel, D. Zsoldos, *Inorg. Chem.* **1997**, *36*, 5384–5389.
[25] a) F. Baumann, W. Kaim, G. Denninger, H.-J. Kümmerer, J. Fiedler, *Organometallics* **2005**, *24*, 1966–1973; b) A. Dogan, B. Sarkar, A. Klein, F. Lissner, Th. Schleid, J. Fiedler, S. Záliš, V. K. Jain, W. Kaim, *Inorg. Chem.* **2004**, *43*, 5973–5980; c) S. Berger, J. Fiedler, R. Reinhardt, W. Kaim, *Inorg. Chem.* **2004**, *43*, 1530–1538.
[26] F. Paolucci, M. Marcaccio, C. Paradisi, S. Roffia, C. A. Bignozzi, C. Amatore, *J. Phys. Chem. B* **1998**, *102*, 4759–4769.
[27] a) C. Amatore, A. Jutand, *Acc. Chem. Res.* **2000**, *33*, 314–321; b) C. Amatore, A. Jutand, *J. Am. Chem. Soc.* **1991**, *113*, 2819–2825.
[28] A. S. Baranski, W. R. Fawcett, C. M. Gilbert, *Anal. Chem.* **1985**, *57*, 166–170.
[29] a) R. Poli, *Chem. Rev.* **1996**, *96*, 2135–2204; b) R. Poli, *Acc. Chem. Res.* **1997**, *30*, 494–501; c) H. Urtel, C. Meier, F. Eisenträger, F. Rominger, J. P. Joschek, P. Hofmann, *Angew. Chem. Int. Ed.* **2001**, *40*, 781–784; d) P. H. M. Budzelaar, N. N. P. Moonen, R. De Gelder, J. M. M. Smits, A. W. Gal, *Eur. J. Inorg. Chem.* **2000**, 753–769.
[30] T. Muruhashi, T. Nagai, T. Okuno, T. Matsutani, H. Kurosawa, *Chem. Commun.* **2000**, 1689–1690.
[31] T. Tanase, H. Ukaji, Y. Yamamoto, *J. Chem. Soc., Dalton Trans.* **1996**, 3059–3064.
[32] A. R. Brown, Z. Guo, F. W. J. Mosselmans, S. Parsons, M. Schröder, L. J. Yellowlees, *J. Am. Chem. Soc.* **1998**, *120*, 8805–8811.
[33] a) A. Klein, W. Kaim, F. M. Hornung, J. Fiedler, S. Záliš, *Inorg. Chim. Acta* **1997**, *264*, 269–278; b) W. Kaim, A. Klein, *Organometallics* **1995**, *14*, 1176–1186; c) A. Klein, W. Kaim, E. Waldhoer, H.-D. Hausen, *J. Chem. Soc., Perkin Trans. 2* **1995**, 2121–2126; d) A. Klein, E. J. L. McInnes, T. Scheiring, S. Záliš, *J. Chem. Soc., Faraday Trans.* **1998**, 2979–2984.
[34] A. Klein, M. Niemeyer, *Z. Anorg. Allg. Chem.* **2000**, *626*, 1191–1195.
[35] M. Krejčík, S. Záliš, M. Ladwig, W. Matheis, W. Kaim, *J. Chem. Soc., Perkin Trans. 2* **1992**, 2007–2010.
[36] P. J. Alonso, L. R. Falvello, J. Fornies, A. Martin, B. Menjon, G. Rodriguez, *Chem. Commun.* **1997**, 503–504.
[37] D. M. Grove, G. van Koten, P. Mul, R. Zoet, J. G. M. van der Linden, J. Legters, J. E. J. Schmitz, N. W. Murrall, A. J. Welch, *Inorg. Chem.* **1988**, *27*, 2466–2473.
[38] H.-J. Krüger, G. Peng, R. H. Holm, *Inorg. Chem.* **1991**, *30*, 734–742.
[39] T. J. Collins, T. R. Nichols, E. S. Uffelman, *J. Am. Chem. Soc.* **1991**, *113*, 4708–4709.
[40] X. Ottenwaelder, R. Ruiz-Garcia, G. Blondin, R. Carasco, J. Cano, D. Lexa, Y. Journaux, A. Aukauloo, *Chem. Commun.* **2004**, 504–505.
[41] M. Krejčík, M. Daňek, F. Hartl, *J. Electroanal. Chem.* **1991**, *317*, 179–187.

Received: September 15, 2006
Published Online: January 19, 2007

